Supplementary Material for:

Bacillithiol is a major buffer of the labile zinc pool in *Bacillus subtilis*

Zhen Ma, Pete Chandrangsu, Tyler C. Helmann, Adisak Romsang, Ahmed Gaballa, John D. Helmann

Includes Figures S1 – S8.

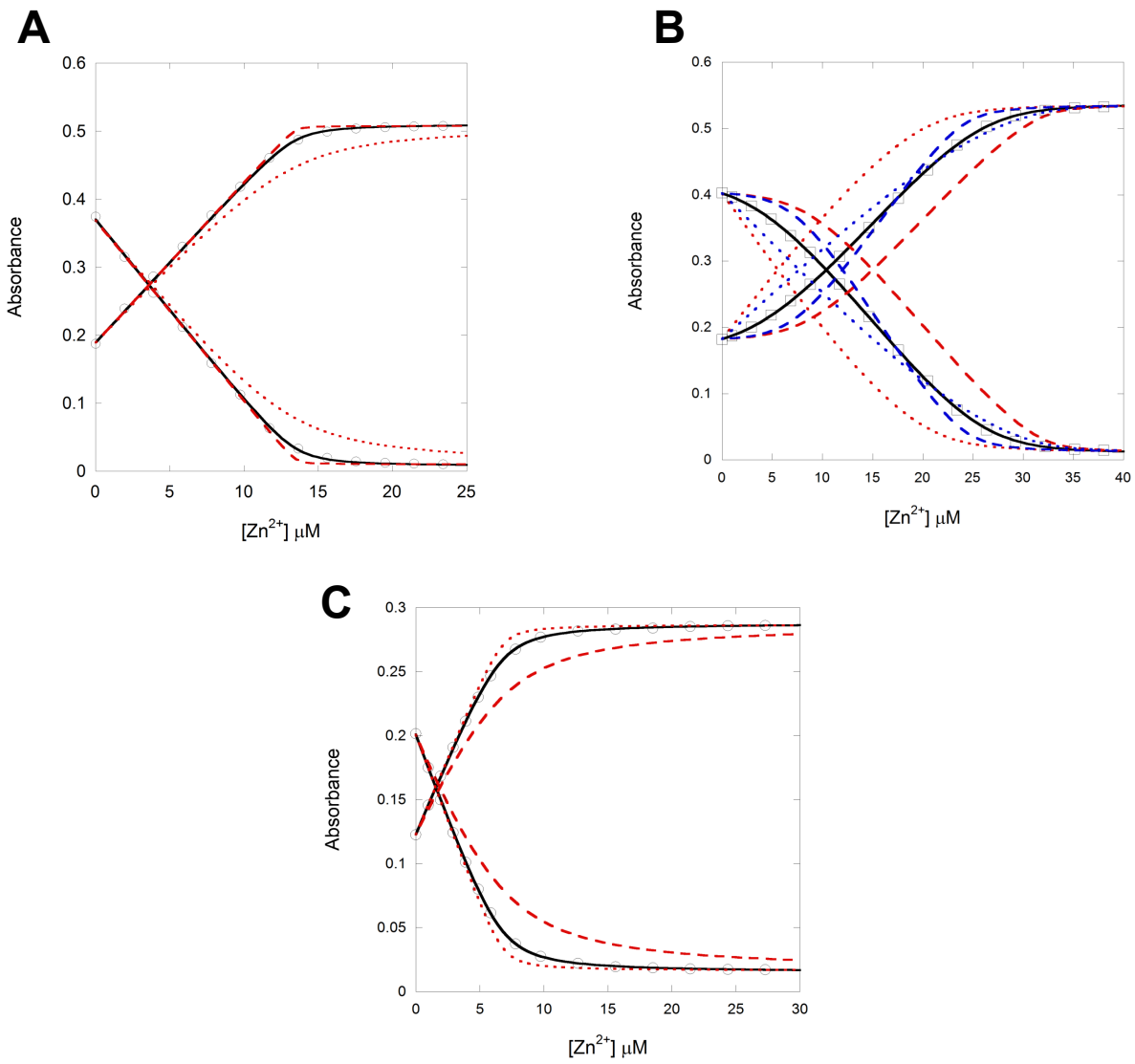

Fig. S1- BSH binds Zn with high affinity. (A) Zn binding to MF2 only. Circles are experimental data. Black curves are fitting curves. Red curves represents simulated curves with 10-fold higher (dash) or lower (dot) binding constant. (B) Zn binding to MF2+BSH. Squares are experimental data. Black curves are fitting curves. Red curves represents simulated curves with 10-fold higher (dash) or lower (dot) K_1. Blue curves represents simulated curves with 10-fold higher (dash) or lower (dot) K_2. (C) Zn binding to MF2+BSSB. Circles are experimental data. Black curves are fitting curves. Red curves represents simulated curves with 10-fold higher (dash) or lower (dot) binding constant.

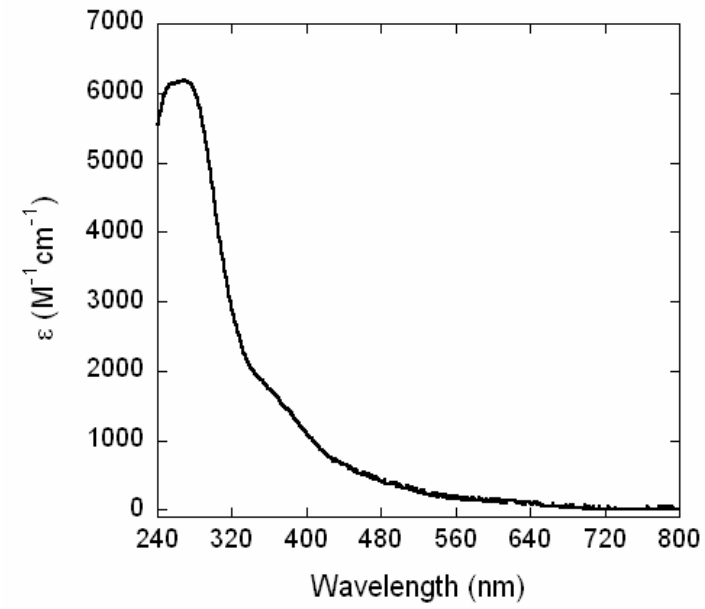

Fig. S2- The BSH thiolate moiety is involved in metal coordination.
Absorption spectrum of $Co(BSH)_2$ complex revealed LMCT in the UV region.

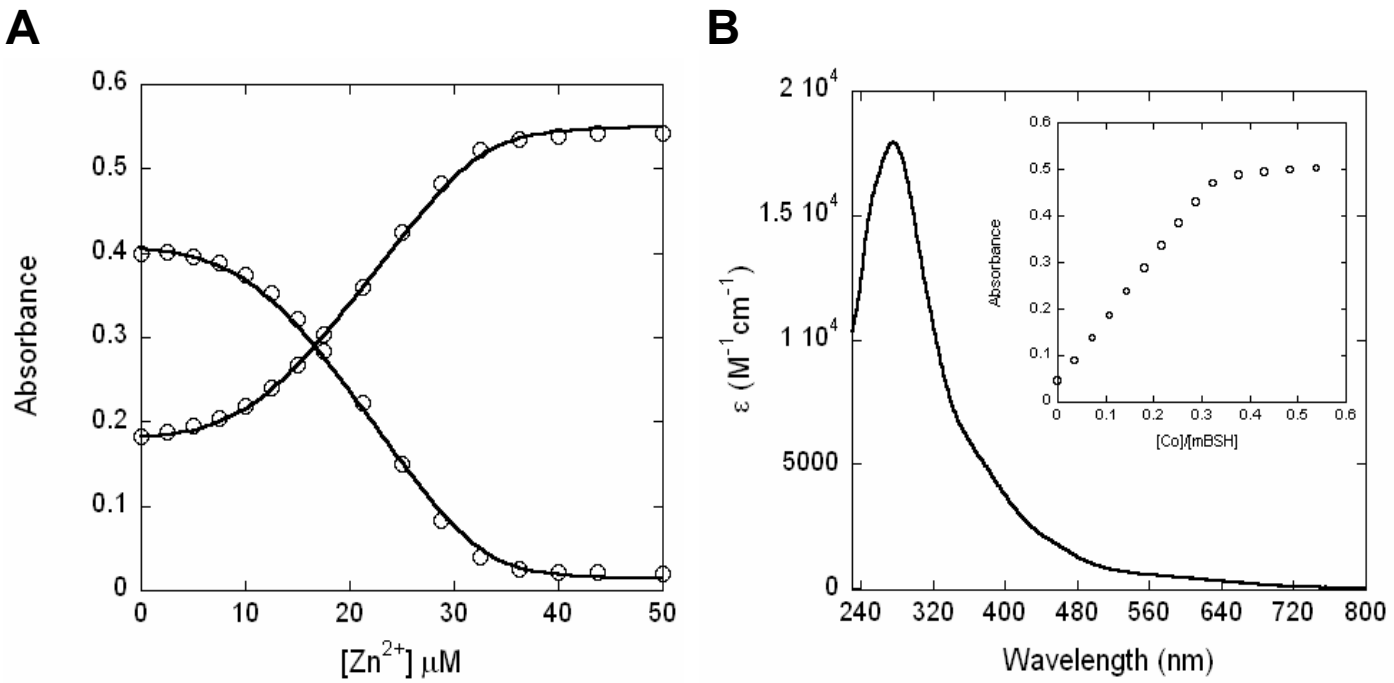

Fig. S3- The BSH carboxylates are involved in Zn^{2+} coordination. (A) The BSH derivative MeO-GlcN-Cys forms a 3:1 complex with Zn^{2+} with an accumulative binding constant β_3 of 3.0 x 10^{16} M^{-3} as determined by the Magfura-2 competition assay (20 mM HEPES, pH 7.7, 0.15 M NaCl, 0.1 mM TCEP). Zn^{2+} titrated into a mixture of 13.5 μM Magfura-2 and 61.5 μM mBSH. (B) The MeO-GlcN-Cys thiolate is involved in coordination as revealed by the observed LMCT.

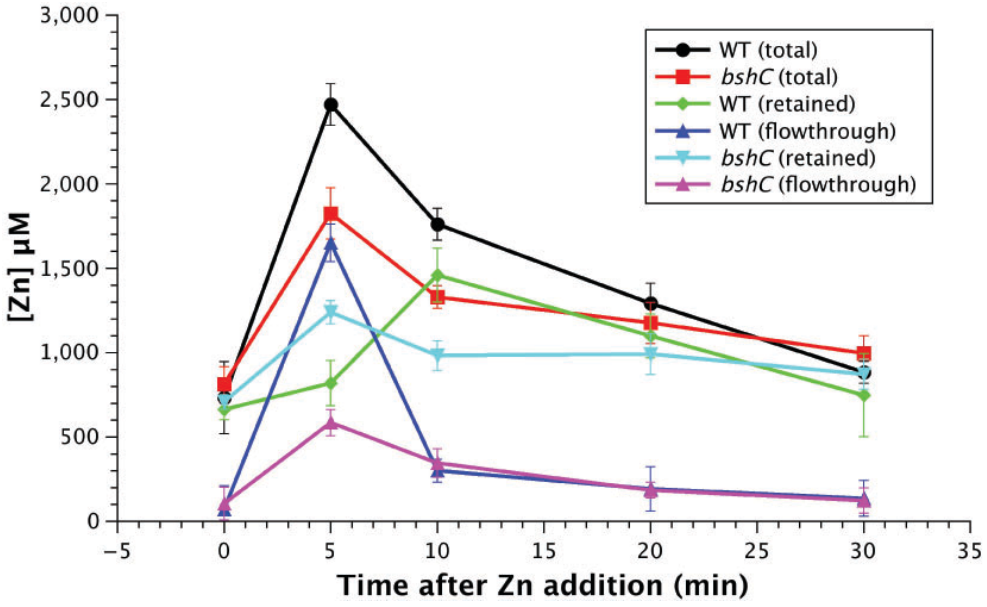

Fig. S4- The major low molecular weight Zn(II) pool is associated with BSH. Wild type and *bshC* null strains were grown in LB until mid-log phase. 200 µM of Zn was added at time 0 and cells were harvested at the indicated times after Zn addition. Cell were lysed and the lysates were passed through a 3 kd Amicon ultracentrifugation column. The Zn concentration of the retentate (> 3kD) and the flowthrough (<3kD) fractions were measured by ICP-MS.

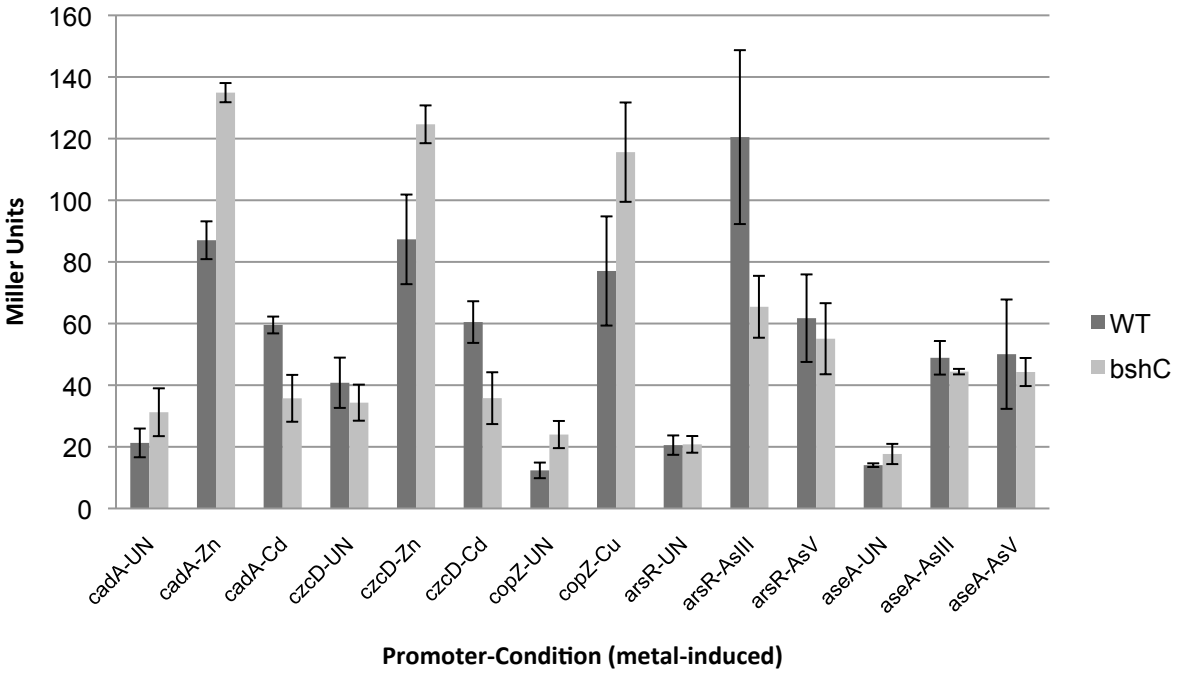

Fig. S5- Effects of BSH on metalloregulation. Induction of promoters repressed by CzrA (*cadA* and *czcD*) is greater in response to Zn(II), consistent with Fig. 4) but is greatly reduced in response to Cd(II). CsoR-mediated induction of the *copZA* operon is slightly greater in cells lacking BSH. ArsR mediated induction is reduced for As(III), but not for As(V). Cells were grown in LB medium and subcultured either in LB (uninduced; UN) or LB containing Zn (0.5 mM), Cd (5 μM), Cu (1 mM), As(III) (0.25 mM), or As(V) (0.25 mM) as indicated. β-galactosidase activities were determined after growth to mid-logarithmic phase and are reported as mean and standard deviation of at least three biological replicates.

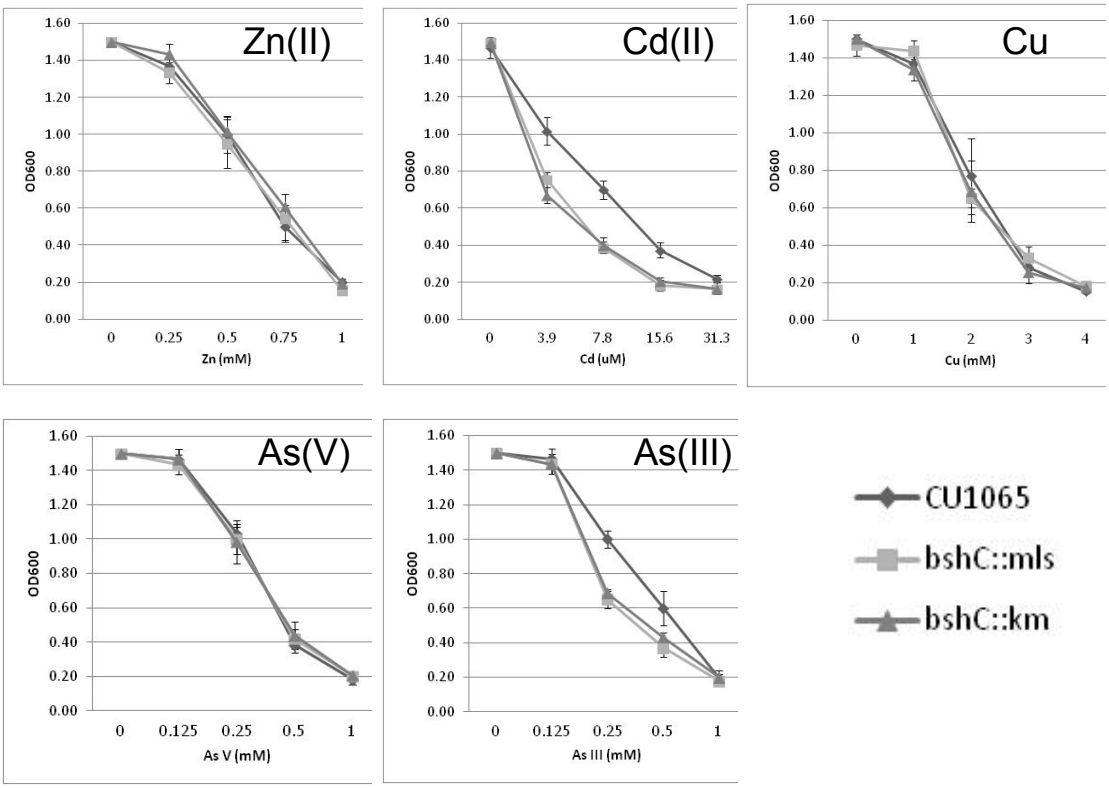

Fig. S6- BSH null mutants have a slightly increased sensitivity to Cd(II) and As(III), but not to other tested metals. Cells were grown in LB containing the appropriate metal at the indicated concentrations overnight at which time the OD_{600} was recorded. The data shown represent the average and standard deviation of three independent experiments.

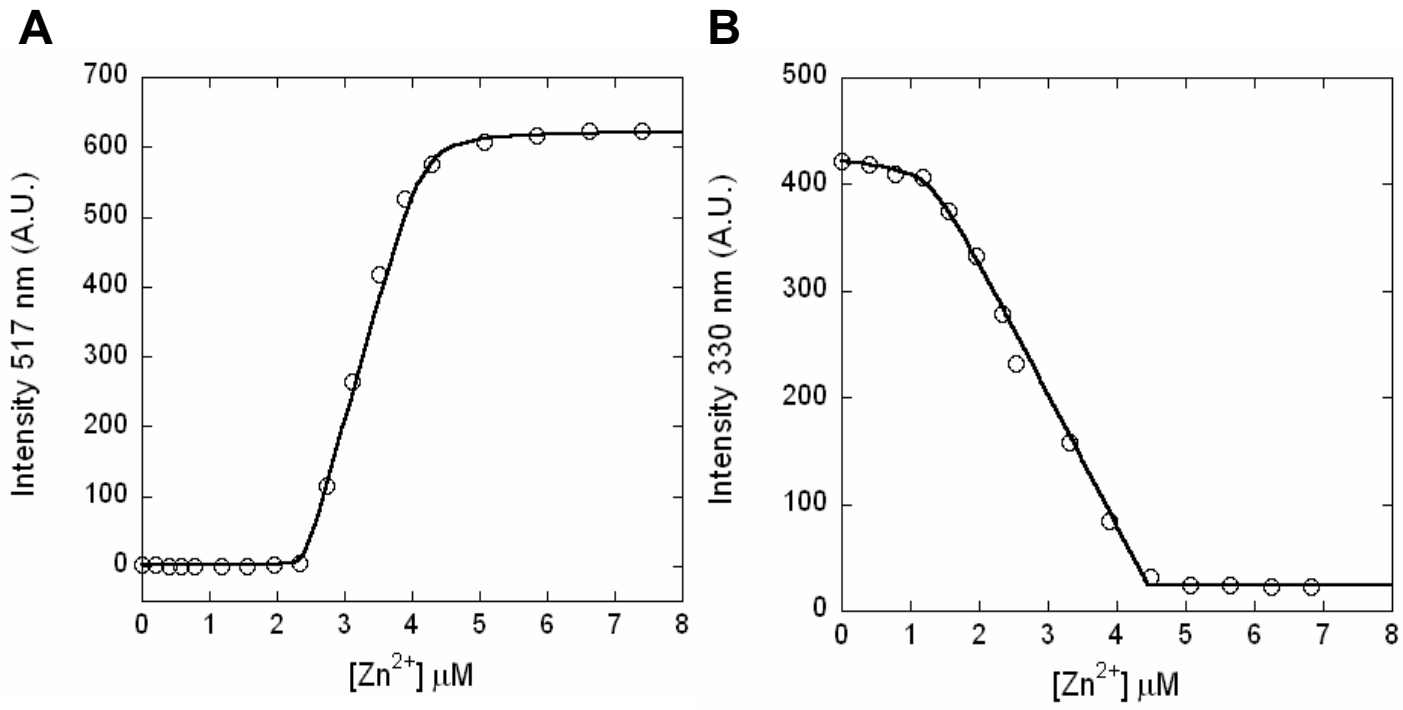

Fig. S7- CzrA binds Zn(II) with high affinity. (A) Zn(II) titrated into 2.4 μM CzrA monomer and 1.8 μM FluoZin-3. (B) Zn(II) titrated into 1.25 μM CzrA monomer and 3.2 μM Quin2 (20 mM Tris, pH 8.0, 0.4 M NaCl). Curves represent the best fit to a competition model involving 1:1 binding of Zn to CzrA monomer. The data indicate that CzrA binds Zn(II) with an affinity of 1.7(±0.2) x 10^{13} M^{-1}. Binding experiments were repeated at least three times and average values and standard deviation are reported.

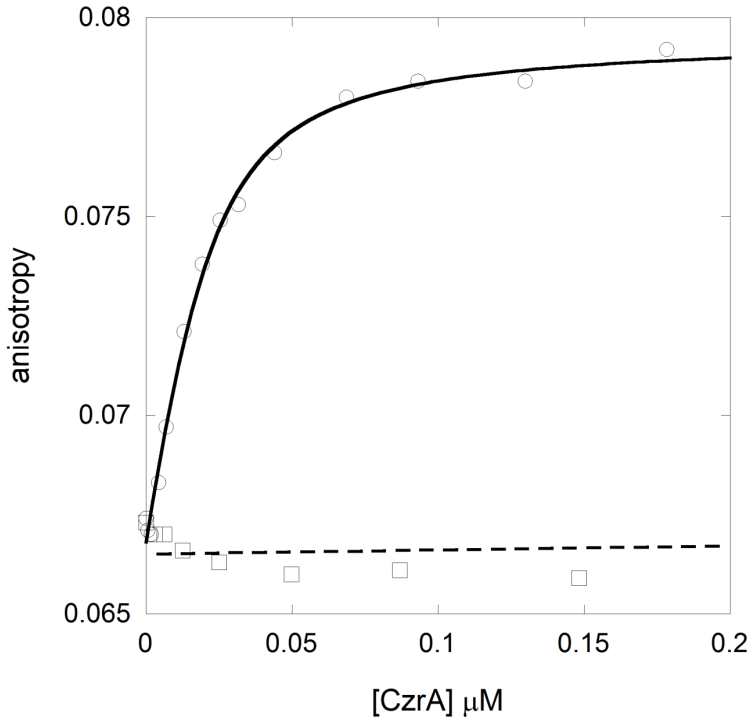

Fig. S8- apo-CzrA binds DNA with high affinity. DNA binding of CzrA with (square, dashed line) or without Zn (circle, solid line). Lines represent the best fit (K_{apo}=2.6(±0.2)x10^8 M^{-1}; $K_{Zn} \leq 10^5$ M^{-1}). Conditions: 20 mM Tris, pH 8.0, 0.4 M NaCl, with 1 mM EDTA or 1 μM Zn.